

## Transport properties of two-dimensional electron gases containing InAs self-assembled dots

G. H. Kim,<sup>a)</sup> D. A. Ritchie, M. Pepper, G. D. Lian, J. Yuan, and L. M. Brown  
*Cavendish Laboratory, University of Cambridge, Madingley Road, Cambridge CB3 0HE, United Kingdom*

(Received 19 May 1998; accepted for publication 26 August 1998)

We present a study of the transport properties of two-dimensional electron gases formed in GaAs/AlGaAs heterostructures in which InAs self-assembled quantum dots have been inserted in the center of a GaAs quantum well. We observed that, while maintaining a constant carrier density, the mobility increased as the InAs dot density was reduced. The ratio of the transport to the quantum lifetime was measured to be approximately five with the dominant scattering mechanism attributed to short-range scattering from the inserted InAs dots. © 1998 American Institute of Physics. [S0003-6951(98)01843-9]

The properties of electrons in one- and zero-dimensional structures have attracted a great deal of interest, both for investigating fundamental physics<sup>1,2</sup> and device applications<sup>3,4</sup> such as quantum dot lasers<sup>5,6</sup> and single electron transistors.<sup>7</sup> However, artificially constructed systems, such as a split gate defined by electron beam lithography, can be constrained by technological limitations. A potentially significant route for the fabrication of one-<sup>8-10</sup> and zero-dimensional<sup>11-13</sup> nanostructures is by natural formation during the growth procedure. For example, self-assembled quantum dots can be created in the Stranski-Krastanov growth mode by growing a highly strained layer above a critical thickness. By employing InGaAs layers grown on (100)GaAs,<sup>14</sup> self-assembled InGaAs dots have recently been realized. Further, in the case of growing InAs on the GaAs substrate, the lattice mismatch is very much higher  $\approx 7\%$  and we have carried out an extensive study to characterize the growth of self-assembled dots.<sup>15</sup>

The experiments presented in this letter determine the transport  $\tau_t$  and quantum  $\tau_q$  life-times of electrons in a GaAs quantum well with inserted InAs dots. Samples are taken from different areas of the same wafer. A sample with no InAs dots is used as a comparison. To illustrate how the disorder introduced by the InAs dots affects the transport and quantum lifetimes, a number of samples with differing InAs dot densities have been studied.

The samples used in this study were grown on undoped GaAs(100) substrates. The structure consisted of a 0.6- $\mu\text{m}$ -thick undoped GaAs buffer layer followed by a 500 Å undoped Al<sub>0.33</sub>Ga<sub>0.67</sub>As barrier, a 200 Å undoped GaAs quantum well, a 400 Å undoped Al<sub>0.33</sub>Ga<sub>0.67</sub>As spacer layer, a 400 Å Si-doped ( $1 \times 10^{18} \text{ cm}^{-3}$ ) Al<sub>0.33</sub>Ga<sub>0.67</sub>As layer, and finally a 170 Å GaAs capping layer.

Within the GaAs quantum well an InAs layer was inserted with a coverage of 2.15 monolayers. The InAs self-assembled quantum dots were covered with either a 50 (wafer C1335) or 100 Å (wafer C1349) GaAs cap grown at a substrate temperature of 530 °C as measured by an optical pyromete. The remainder of the structures were grown at

580 °C. A reference sample (C1127) was also grown with no InAs layer.

All of the devices were processed using standard optical lithography and wet etching into a Hall bar with length 800  $\mu\text{m}$  and width 80  $\mu\text{m}$ . A NiCr/Au gate was deposited to form a surface Schottky gate thereby enabling the two-dimensional electron gas (2DEG) carrier density  $n_s$  to be changed. Standard low frequency lock-in techniques were used to measure the magnetoresistance with a constant current of 100 nA passed between the source and drain.

Figure 1 shows the plan view transmission electron microscopy (TEM) images from wafer C1349. These samples are taken from three different wafer regions, each with different dot densities  $n_d$ . The samples are as follows: C1349c (center of the wafer), C1349m (midway between center and edge), and C1349e (edge of the wafer). There is a factor of two variation in the InAs dot density between the C1349c

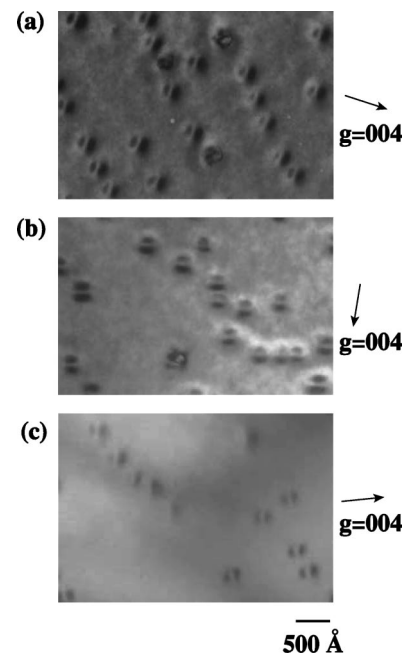


FIG. 1. Plan view TEM images of self-assembled InAs dots on wafer C1349 for three different regions: (a) center, (b) midway between center and edge, and (c) edge.

<sup>a)</sup>Electronic mail: gk10004@cam.ac.uk

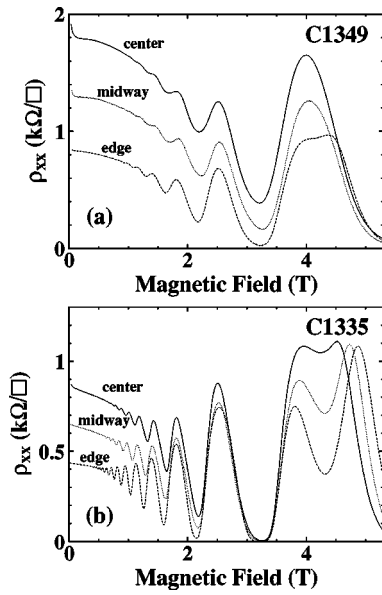


FIG. 2. Comparing the longitudinal resistivity of sample (a) C1349 and (b) C1335 with carrier densities of  $n_s = 2.95 \times 10^{11}$  and  $3.00 \times 10^{11}$   $\text{cm}^{-2}$ , respectively, for three different parts of the wafer: center (solid lines), midway between center and edge (dotted lines), and edge (broken lines).

and C1349e samples. The experimental dot densities for C1349c [Fig. 1(a)], C1349m [Fig. 1(b)], and C1349e [Fig. 1(c)] are  $n_d = 5.8 \times 10^9$ ,  $4.6 \times 10^9$ , and  $2.5 \times 10^9$   $\text{cm}^{-2}$ , respectively, counting from an area of  $12 \mu\text{m}^2$ . The dot density in sample C1335c was  $3.0 \times 10^9$   $\text{cm}^{-2}$ . We find the average dimension of the dots to be  $\sim 360$  Å wide and  $\sim 80$  Å high in sample C1349c, and  $\sim 280$  Å wide and  $\sim 40$  Å high in sample C1335c. All dots show strain contrast, and very few show loss of coherency, as observed.<sup>15</sup>

Magnetoresistance measurements show that the resistivity decreases as the InAs dot density decreases. Figure 2 shows the typical magnetoresistance data for the three different regions of the wafers C1349 and C1335 at  $T = 1.6$  K. As each device has very similar carrier densities the period of the Shubnikov–de Haas (SdH) oscillations remains the same. Here the carrier densities have been determined as  $n_s = 2.95 \times 10^{11}$  [Fig. 2(a)] and  $3.00 \times 10^{11}$   $\text{cm}^{-2}$  [Fig. 2(b)]. For wafer C1349 in Fig. 2(a) the longitudinal resistivity at zero magnetic field increases as the density of InAs dots increases. Consequently the mobility  $\mu$  is higher in sample C1349e than in sample C1349c. However, the zero field resistance, for the same positions on the wafer are approximately twice as large in wafer C1349 as in C1335. This

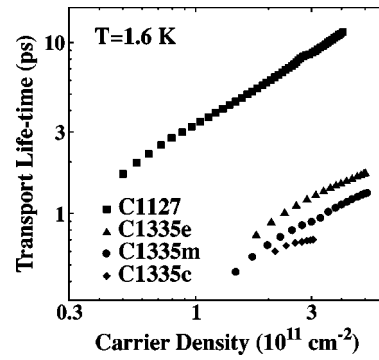


FIG. 3. Transport lifetimes  $\tau_t$  from C1335 and the reference sample C1127 as a function of carrier density  $n_s$  at  $T = 1.6$  K.

implies that the mobilities in C1349 must be approximately half those in C1335. The spin splitting of the SdH oscillations also reflects the sample disorder. For wafer C1335 in Fig. 2(b) the two spin-split peaks at filling factor  $\nu = 3$  ( $B = 4.3$  T) are well resolved in sample C1335e. However, as the sampling point moves towards the center the increasing disorder (InAs dot density) causes a blurring of the spin splitting. Similar behavior, albeit for lower mobilities, is observed in sample C1349.

Negative magnetoresistance is also observed below about 1 T in both wafers C1335 and C1349 as shown in Fig. 2. The amplitude of negative magnetoresistance increases with increase of InAs dot density. This magnetoresistance behavior is more likely due to localization of electrons and back scattering at zero magnetic field in the potential fluctuations of the InAs dots. Such magnetoresistance behavior has also been observed by other authors<sup>16,17</sup> who attributed it to the disorder introduced via the randomness in the position and size of lithographically defined antidots.

Figure 3 shows the transport lifetime as a function of carrier density for samples C1335(c,m,e) and C1127 at 1.6 K. The carrier densities were determined by low-field Hall measurements and the density was varied by applying a front gate voltage. The transport lifetime in the reference sample C1127 is about ten times larger than that of sample C1335 with InAs dots. This extreme reduction in transport lifetime is caused by the inserted InAs dots. For sample C1349, the transport behavior is similar to C1335. Table I shows a summary of the transport characteristics at 1.6 K.

Using the SdH oscillation amplitudes we have determined the quantum lifetimes. The analysis for the quantum lifetimes is similar to that employed by Coleridge *et al.*<sup>18</sup>

TABLE I. Sample characteristics from transport measurements at 1.6 K.  $d_c$  is the thickness of the GaAs capping layer covering the InAs dots. All samples required illumination with a red light-emitting diode to promote conduction.

Wafer	Sample	$\mu$ ( $10^4$ $\text{cm}^2/\text{V s}$ )	$n_s$ ( $10^{11}$ $\text{cm}^{-2}$ )	$\tau_t$ (ps)	$\tau_q$ (ps)	$n_d$ ( $10^9$ $\text{cm}^{-2}$ )	$d_c$ (Å)
C1127	...	18.48	2.52	6.85	0.41	...	...
C1335	edge	4.70	3.00	1.79	0.37	...	50
C1335	middle	3.20	3.00	1.22	0.26	...	50
C1335	center	2.40	3.00	0.91	0.22	3.0	50
C1349	edge	2.50	2.95	0.95	0.13	2.5	100
C1349	midway	1.50	2.95	0.57	0.10	4.6	100
C1349	center	1.10	2.95	0.41	0.08	5.8	100

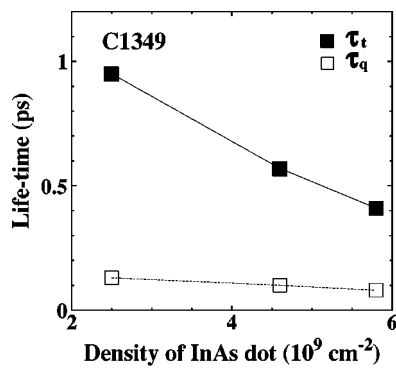


FIG. 4. Summary of the transport  $\tau_t$  and quantum  $\tau_q$  lifetimes from wafer C1349. The lifetimes are plotted as function of the InAs dot density.

Figure 4 shows both the transport and quantum lifetimes plotted against InAs dot density for wafer C1349, where the InAs dot densities were determined from TEM images. The quantum lifetime decreases when the InAs dot density increases, and remains five times smaller than the transport lifetime. For a high mobility 2DEG formed in GaAs/AlGaAs heterostructures, the ratio of transport and quantum lifetimes was observed to be greater than 10.<sup>19</sup> This is indicative that the dominant scattering mechanism involves long-range scattering from remote ionized impurities. In contrast to the GaAs/AlGaAs heterojunctions, the SiO<sub>2</sub>/Si interface in metal-oxide semiconductor field effect transistors (MOSFETs) is very rough, and the transport and quantum lifetimes are almost the same, as interface roughness scattering is the predominant scattering mechanism.<sup>20–22</sup> In our sample the transport to quantum lifetime ratio lies between the values for high mobility GaAs/AlGaAs heterojunctions and MOSFETs and is a result of the short-range scattering due to the inserted InAs dots.

In summary, we have investigated the transport and quantum lifetimes in GaAs quantum wells containing InAs self-assembled dots. The InAs dot density was varied by approximately a factor of two from the edge to the center of the wafer, thereby increasing the disorder. The transport to quantum lifetime ratio was observed to be approximately five and was independent of the InAs dot density. A study of the

quantum and transport lifetimes showed that both lifetimes varied strongly across the wafer, and that the dominant scattering mechanism was short-range scattering from InAs dots.

We wish to thank the Engineering and Physical Sciences Research Council (UK) for supporting this work. G.H.K. acknowledges support from Arkinson Fund, Clare College, D.A.R. acknowledges support from Toshiba Cambridge Research Center, and G.D.L. acknowledges support from the Royal Society.

- <sup>1</sup>J.-Y. Marzin, J.-M. Gérard, A. Izraël, and D. Barrier, *Phys. Rev. Lett.* **73**, 716 (1994).
- <sup>2</sup>H. Drexler, D. Leonard, W. Hansen, J. P. Kotthaus, and P. M. Petroff, *Phys. Rev. Lett.* **73**, 2252 (1994).
- <sup>3</sup>H. Sakaki, G. Yusa, T. Someya, Y. Ohno, T. Noda, H. Akiyama, Y. Kadoya, and H. Noge, *Appl. Phys. Lett.* **67**, 3444 (1995).
- <sup>4</sup>K. Imamura, Y. Sugiyama, Y. Nakata, S. Muto, and N. Yokoyama, *Jpn. J. Appl. Phys., Part 2* **34**, L1445 (1995).
- <sup>5</sup>S. Fafard, K. Hinzer, S. Raymond, M. Dion, J. McCaffrey, Y. Feng, and S. Charbonneau, *Science* **274**, 1350 (1996).
- <sup>6</sup>F. Heinrichsdor, M.-H. Mao, N. Kirstaedter, A. Krost, D. Bimberg, A. O. Kosogov, and P. Werner, *Appl. Phys. Lett.* **71**, 22 (1997).
- <sup>7</sup>K. Yano, T. Ishii, T. Kobayashi, F. Murai, and K. Seki, *IEEE Trans. Electron Devices* **41**, 1628 (1994).
- <sup>8</sup>P. M. Petroff, A. C. Gossard, and W. Wiegmann, *Appl. Phys. Lett.* **45**, 620 (1984).
- <sup>9</sup>M. Tanaka and H. Sakaki, *Appl. Phys. Lett.* **54**, 1326 (1989).
- <sup>10</sup>R. Nötzel, J. Temmyo, and T. Tamamura, *Appl. Phys. Lett.* **64**, 3557 (1994).
- <sup>11</sup>T. Noda, M. R. Fahy, T. Matsusue, B. A. Joyce, and H. Sakaki, *J. Cryst. Growth* **127**, 783 (1993).
- <sup>12</sup>D. Leonard, K. Pond, and P. M. Petroff, *Phys. Rev. B* **50**, 11687 (1994).
- <sup>13</sup>M. Grundmann, O. Stier, and D. Bimberg, *Phys. Rev. B* **52**, 11969 (1995).
- <sup>14</sup>D. Leonard, M. Krishnamurthy, C. M. Reaves, S. P. Den-Baars, and P. M. Petroff, *Appl. Phys. Lett.* **63**, 3203 (1993).
- <sup>15</sup>G. D. Lian, J. Yuan, L. M. Brown, G. H. Kim, and D. A. Ritchie, *Appl. Phys. Lett.* **73**, 49 (1998).
- <sup>16</sup>G. M. Gusev, P. Basmaji, Z. D. Kvon, L. V. Litvin, Y. V. Nastaushev, and A. I. Toropov, *Surf. Sci.* **305**, 443 (1994).
- <sup>17</sup>F. Nihey, M. A. Kastner, and K. Nakamura, *Phys. Rev. B* **55**, 4085 (1997).
- <sup>18</sup>P. T. Coleridge, R. Stoner, and R. Fletcher, *Phys. Rev. B* **39**, 1120 (1989).
- <sup>19</sup>J. P. Harrang, R. J. Higgins, R. K. Goodall, P. R. Jay, M. Laviron, and P. Delescluse, *Phys. Rev. B* **32**, 8126 (1985).
- <sup>20</sup>F. F. Fang, A. B. Fowler, and A. Hartstein, *Phys. Rev. B* **16**, 4446 (1977).
- <sup>21</sup>F. Stern and W. E. Howard, *Phys. Rev.* **163**, 816 (1967).
- <sup>22</sup>T. Ando, A. B. Fowler, and F. Stern, *Rev. Mod. Phys.* **54**, 437 (1982).